

Modelling and analysis of cutting forces while micro end milling of Ti-alloy using finite element method

Narendra Bhople¹, Sachin Mastud^{2,*}, and Satish Satpal³

¹ Department of Production Engineering, VJTI, Mumbai, India

² Department of Mechanical Engineering, VJTI, Mumbai, India

³ Department of Mechanical Engineering, NTC, Pune, India

Received: 22 August 2021 / Accepted: 10 October 2021

Abstract. Micromilling is one of the preferable micro-manufacturing process, as it exhibits the flexibility to produce complex 3D micro-parts. The cutting forces generated in micro end milling can be attributed for tool vibration and process instability. If cutting forces are not controlled below critical limits, it may lead to catastrophic failure of tool. Cutting force has a significant role to decide the surface roughness. Therefore accurate prediction of cutting forces and selection of suitable cutting parameters mainly feed, is important while micro end milling. In present study, finite element method (FEM) based model has been developed by using ABAQUAS/Explicit 6.12 software. Von-Misses stresses and cutting forces are predicted while micro end milling of Ti-6Al-4V. Further, cutting forces were measured during experimentation using dynamometer mounted on micro-milling test bed. Cutting forces predicted by FEM model are in good agreement with the experimental force values. Obtained FEM results have been used to study the size effect in micro end milling process. Moreover, the effect of uncut chip thickness to cutting edge radius ratio (h/rc) on surface roughness (Ra) has been studied. It is found the feed $2.5 \mu\text{m}/\text{tooth}$ is suitable value to produce optimum surface roughness and cutting forces.

Keywords: Cutting force / finite element method / micro-end milling / tungsten carbide / Von-Misses stress / surface roughness / Ti-6Al-4V

1 Introduction

Micromilling process is more versatile than competing micromachining processes such as micro EDM. Micro-milling can produce 3D shapes on metallic alloys, ceramics and polymers [1]. It is extensively used in micro manufacturing of components required in electronics, defence, telecommunications, mechatronics and biomedical sectors [2]. This process is faster as well cost effective compared to other micro manufacturing process [3,4]. Micromilling provides higher material removal rates as well as machining of high aspect ratio parts can be realized via this process [5]. Size effect, minimum chip thickness and material inhomogeneity are some of the issues in micro-milling. The assumption made in conventional Merchant's theory (cutting edge is sharp and there is no workpiece-tool contact along clearance face) are invalid in the micro milling process. Identification of minimum chip thickness values for different work material is additional challenge in micromilling. Lower undeformed chip thickness may increase cutting forces by ploughing mechanism while

higher undeformed chip thickness increases cutting forces by increasing chip load.

Performance of micro end milling is significantly affected by the cutting forces; high cutting forces are attributed to the tool deflection and process instability (tool run out, chatter). High cutting forces are very prevalent while machining harder materials like titanium alloys and hardened steel. Catastrophic failure of tool may also occur if cutting forces are not optimized, as micro tools has low stiffness. Large negative rake angle due to tool wear and elasto-plastic deformation of workpiece contributes to higher cutting forces [5–8]. Prediction of cutting forces is essential in micro end milling to improve product quality and to reduce machining cost. The h/rc ratio is crucial parameter in micromilling. This factor is characteristics of a given material at specified cutting conditions. Balazs et al. [8] presented the valuable findings of micromilling in their latest review article. In micro milling, the value of undeformed chip thickness is equivalent to the cutting edge radius of tool and the grain size of workpiece. Therefore, the lower uncut chip thickness affects the surface quality by accelerating the ploughing mechanism. It is also suggested that increased feed per tooth has positive effect on tool condition.

* e-mail: samastud@me.vjti.ac.in

Industries are using predictive modelling of machining process. These modelling techniques are classified as numerical, analytical, experimental, hybrid and artificial intelligent based models. Fundamental machining processes parameters like stress distribution, cutting forces, strain and temperature can be predicted by using these modelling techniques. Mechanistic modelling can also be used to predict the cutting forces in micro end milling with due consideration of tool geometry and material removal mechanism. 2-D Finite element method based modelling techniques are widely accepted in mechanical microcutting due to their good computational speed [9–11]. FEM can model a micro cutting operation to predict how all process variables influence the desired responses. It has been extensively used to predict the cutting forces, chip formation and tool wear.

Thepsonthi and Ozel [12] used 3 D FE process to simulate chip flow and tool wear while machining Ti-6Al-4V for different cutting edge radii. The effect of tool edge radius wear on the performance of micro-end milling process has been studied by full-immersion, half immersion, up and down milling approaches. To study the temperature dependent softening effects the modified Johnson-Cook (J-C) material model was used to model the Ti-6Al-4V workpiece. Further they compared the results obtained in 3-D FEM and 2-D FEM process by using five degree polynomial equation with curve fitting. The increased cutting edge radius ($3\ \mu\text{m}$ to $6\ \mu\text{m}$ to $12\ \mu\text{m}$) significantly affected the milling process, in terms of increased tool wear, higher cutting forces and cutting temperature. Higher tool wear in up milling has been observed as the edge radius increases compared to down milling, in down milling tool enters in the workpiece at the maximum chip thickness this easily shears the workpiece and produce chip. Further less ploughing in down milling reported by authors. The cutting forces and tool wear obtained in 2-D FEM are in good agreement with 3-D FEM. As per author suggestions, 2-D FEM can be used to predict the cutting forces and tool wear instead of 3-D FEM. As 3-D FEM takes more computational time and it needs high configured system. Davoudinejad et al. [13] predicted the cutting forces, chip flow and burr formation by using 3-D FEM while micro-milling of aluminium 6061-T6. In this study Power Law constitutive model has been used to calculate the flow stress. Model shows the good predictability in terms of chip shape and burr formation while over estimation of cutting forces has been reported. The overestimated cutting forces by FEM simulation attributed to modeling of micro milling in ideal condition, lack of information on the machined material constitutive model inside the FEM and inappropriate selection of friction coefficient. Author suggested the improvement needed in used material model or Johnson-Cook constitutive model can be used with proper material constants for Al6061-T6.

Pratap and Patra [14] used FEM based modelling to predict the cutting forces while micromilling oxygen free highly conductive copper. ABAQUS/Explicit 6.12 software has been used to predict the forces with due consideration to thermo mechanical properties, tool edge radius effect and failure parameters of the workpiece. It is

found that the tangential and feed force increases with increase in chip load. Further, specific cutting forces increases with decrease in feed. Thepsonthi and Ozel [15] used FEM to compare the result by using two different material assumptions namely viscoplastic and elasto-viscoplastic while micro end milling of Ti-6Al-4V. In elasto-viscoplastic model, serrated chip formation takes place. It took 8.3 times more duration for the computation compared to the viscoplastic model. However, material assumption has not significantly affected the magnitude of predicted cutting forces. To predict the tool wear, viscoplastic FEM model is sufficient.

Attanasio et al. [16] used FEM to examine the results obtained with and without tool run out while micromilling of CuZn37 brass. It is found that the cutting forces are significantly affected by tool run-out. Qualitative comparison of predicted chip shape, chip flow is in close agreement with the chips produced in machining. Wang et al. [17] used finite element simulation to predict machining forces while working on inconel 718. It is found that the minimum uncut chip thickness for inconel 718 is at Feed = $1.5\ \mu\text{m}/\text{tooth}$. Further, they suggested to provide feed higher than critical value. Pratap and Patra [18] analyzed cutting forces while micro end milling Ti-6Al-4V by using FEM. Johnson-Cook material model with material damage initiation criteria has been used for modelling. Experimental and simulated cutting forces are found in good agreement. The value of Von-Misses stress and cutting temperature are higher than macro milling, this attributed to the low feed values and effect of tool edge radius. Jin and Altintas [19] predicted micro-milling forces with finite element method while processing brass 260. They initially obtained the cutting force coefficient with FE simulations, by using different cutting edge radii and chip loads. Further the force coefficient was used to simulate micro milling forces. A good predictability for normal cutting force while less accuracy for thrust force is reported in their study.

Ti-6Al-4V is ‘workhorse’ alloy for aerospace applications [20]. The demand of Ti-6Al-4V has been increasing in automotive, power, marine, aeronautic and especially in the medical field from last decade. This is alloy of $\alpha + \beta$ group with good corrosion resistance, high strength to weight ratio and better biocompatibility. Processing of this alloy is difficult due to its lower thermal conductivity, high friction coefficient and excessive tool wear [21,22]. Formation of built up edge is very common while machining Ti-6Al-4V. High cutting speed while machining Ti alloy causes increase in cutting zone temperature this leads to accelerate diffusion wear [2,23]. Overall, it has been found that the inappropriate selection of cutting parameters, mainly feed significantly affects the cutting forces, surface roughness and tool wear. It is also keenly noted that the results obtained by 2-D FE simulation are matching at satisfactory level with 3-D FE simulation in terms of cutting forces and tool wear. Ti-6Al-4V has wide use to produce micro systems and limited literature has been found related to selection of h/rc ratio for Ti-6Al-4V. Therefore, in present study 2-D FEM is used to predict the Von-Misses stresses and cutting forces in micro end milling process. Further, the size effect and the effect of different h/rc ratio on surface roughness has also been

studied by measuring surface roughness of machined slots. Micro slots with 20 mm length are cut in Ti-6Al-4V material by using 800 μm diameter tungsten carbide end mill with cutting edge radius 2 μm. The validity of proposed model is checked by comparing the simulated cutting forces with experimental values, good predictability of the proposed model has been found. Trend suggests a size effect at lower feed values. It is found the provided feed /tooth slightly higher than cutting edge radius produce better surface finish, in present work the feed 2.5 μm/tooth is identified to optimize the cutting forces and surface roughness.

2 FEM modelling of micro end milling

A finite element method based micro end milling model for Ti-6Al-4V has been developed by using ABAQUS/Explicit 6.12 software. In proposed model the dynamic, explicit and adiabatic condition has been used to analyse the cutting process. FEM has ability to predict cutting forces, chip formation, tool temperature and stress distribution for various cutting condition. The orthogonal micro cutting process with tool-workpiece interaction is shown in Figure 1.

In Figure 1, h represents the uncut chip thickness and r is the edge radius. The point RP represents the reference point to collect the data, tool used for modelling considered as an isothermal rigid body. The initial temperature of tool and workpiece material considered was 298 °K (Room temperature) and dry cutting environment (no lubrication) considered while modelling. In present study, tool can move in X direction while workpiece is fixed in a fixture. Accuracy of simulation is ensured by using mesh size comparable to tool edge radius. The flowchart to predict the cutting forces and Von-Misses stress in micro end milling process by using ABAQUS shown in Figure 2.

2.1 Material behaviour modelling and properties

Johnson and Cook (J and C) constitutive model has been used in proposed FEM simulation of orthogonal micro end milling process. Equation 1 represent the coupled effect of strain (term1), strain rate (term2) and temperature (term 3) on flow stress of the material (σ) [9].

$$\sigma = [A + B(\epsilon)^n] \left[1 + C \ln \left(\frac{\dot{\epsilon}}{\dot{\epsilon}_0} \right) \right] \left[1 - \left(\frac{T - T_0}{T_m - T_0} \right)^m \right] \quad (1)$$

$$\epsilon_{failure} = \left[d_1 + d_2 \exp \left(d_3 \frac{P}{\bar{\sigma}_{jc}} \right) \right] \left[1 + d_4 \ln \left(\frac{\dot{\epsilon}}{\dot{\epsilon}_0} \right) \right] \times \left[1 + d_5 \left(\frac{T - T_0}{T_m - T_0} \right)^m \right] \quad (2)$$

In equation (1) parameters A , B and n represent the yield strength, strain hardening constant and strain hardening coefficient of the material respectively. C is strengthening coefficient of strain rate ϵ is the true strain, $\dot{\epsilon}$ and $\dot{\epsilon}_0$ represent equivalent and reference plastic strain

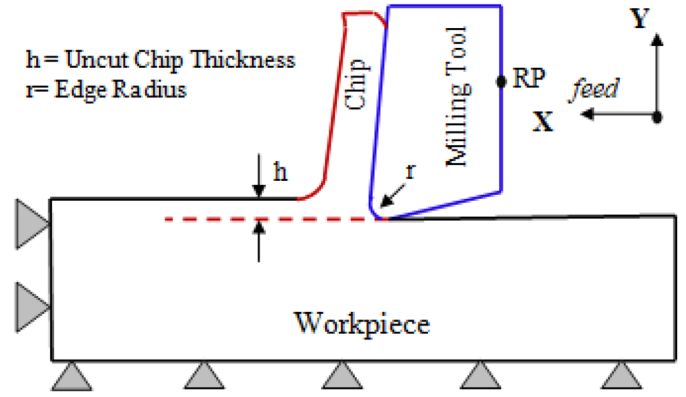


Fig. 1. Finite element model of micro end milling process.

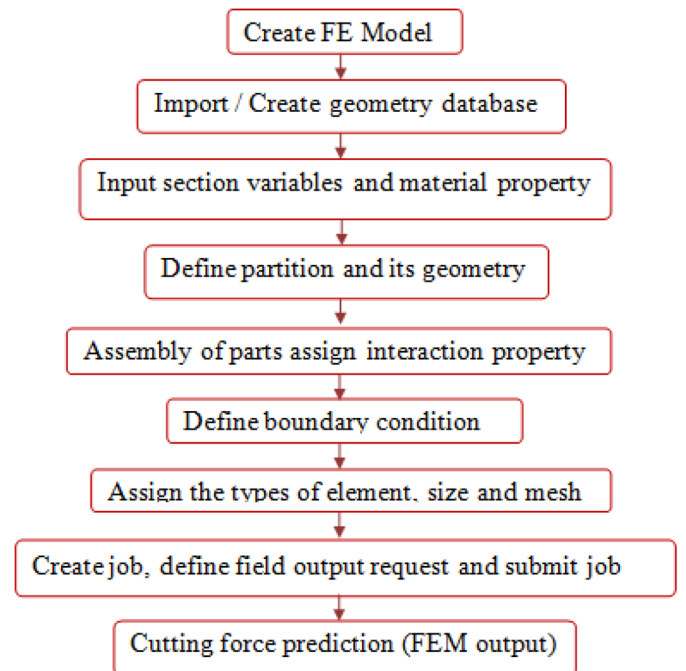


Fig. 2. Finite element model flowchart to predict the cutting forces.

rates. T , T_m and T_0 are the cutting zone, melting and room temperatures respectively. Whereas, m is the thermal softening index. Table 1 shows the Johnson-Cook model parameters and mechanical properties of Ti-6Al-4V used in FEM modelling. Equation (2) shows the influence of strain, strain rate and temperature on the calculation of fracture strain of the material. Failure parameters i.e. d_1 - d_5 represent the initial failure strain, exponential factor, triaxiality factor, strain rate factor and temperature factor respectively. Failure parameters for Ti-6Al-4V are given in Table 2. In the present model, if average plastic strain reaches the critical value, the material considers as failed and it will be eliminated at next solver step.

Table 1. Johnson-Cook parameters and mechanical properties of Ti-6Al-4V [24].

A (Mpa)	B (Mpa)	n	C	m	Density (kg/m ³)	Elastic modulus (Mpa)	Poissons ratio	Hardness (HRC)	T (room)	T (melting)
1000	780	0.47	0.033	1.02	4430	123	0.34	32	20°	1605°

Table 2. Johnson-Cook failure parameter of Ti-6Al-4V alloy [24].

d1	d2	d3	d4	d5
-0.09	0.25	-0.5	0.014	3.87

2.2 Material removal mechanism

In micro milling, uncut chip thickness increases from zero to feed per flute. Tool edge radius has strong relationship with material removal mechanism. The probability of elastic deformation in micromachining is considerably higher than macromachining. For the commencement of chip, the value of feed and depth of cut should be higher than critical chip thickness called as minimum chip thickness [5]. If the ratio of uncut chip thickness to cutting edge radius is less than unity, it causes ploughing (elastic deformation of material increase cutting forces) while more than unity values promotes the chip formation. However, higher ratios of uncut chip thickness to cutting edge radius can increase cutting forces by increasing chip load. Equation (3) shows that in micro end milling, the uncut chip thickness (h) is associated with feed per tooth (f_t) and rotation angle (φ). The direction of cutting forces in micro end milling for two fluted end mill shown in Figure 3. F_y and F_x represent the cutting force normal to feed and along feed direction respectively, Whereas f_t is feed per tooth. dF_f and dF_t represent the feed force and tangential force respectively. Equation (3) and Figure 3 shows in micro milling h is directly associated with f_t .

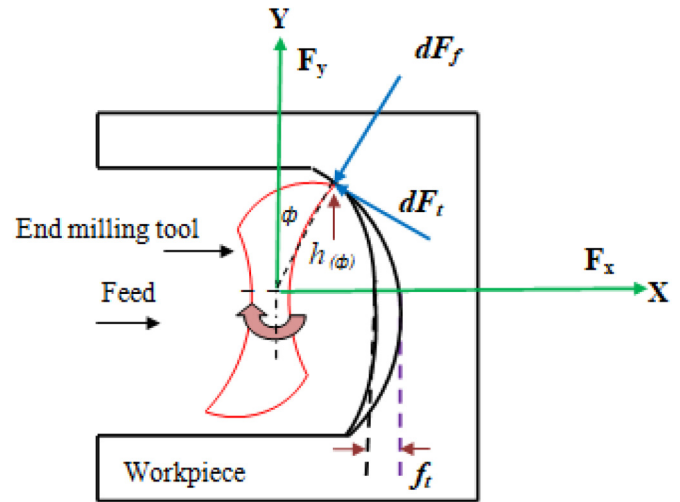
$$h(\varphi) = f_t \sin(\varphi) \quad (3)$$

2.3 FEM simulation of cutting forces

Micro end milling process simulation has been performed for nine numbers of runs, by using tungsten carbide end mill having diameter 800 μm and cutting edge radius 2 μm . The feed rate is varied keeping all other parameters constant. Moreover, variations in Von-Misses stress, tangential force, feed force and specific cutting force are analysed with respect to feed. The cutting simulation parameters are shown in Table 3.

In FEM based simulation, yield criteria and fatigue strength of the material are estimated by analysing Von-Misses stresses. Figure 4 shows simulated result of Von-Misses stress distribution for the feed 0.5 $\mu\text{m}/\text{tooth}$, 3 $\mu\text{m}/\text{tooth}$, 6 $\mu\text{m}/\text{tooth}$ respectively.

From Figure 5, it is found that at the lower values (0.5–1.5 $\mu\text{m}/\text{tooth}$) cutting tool experienced more difficulty for the chip formation. Moreover, the Von-Misses stress

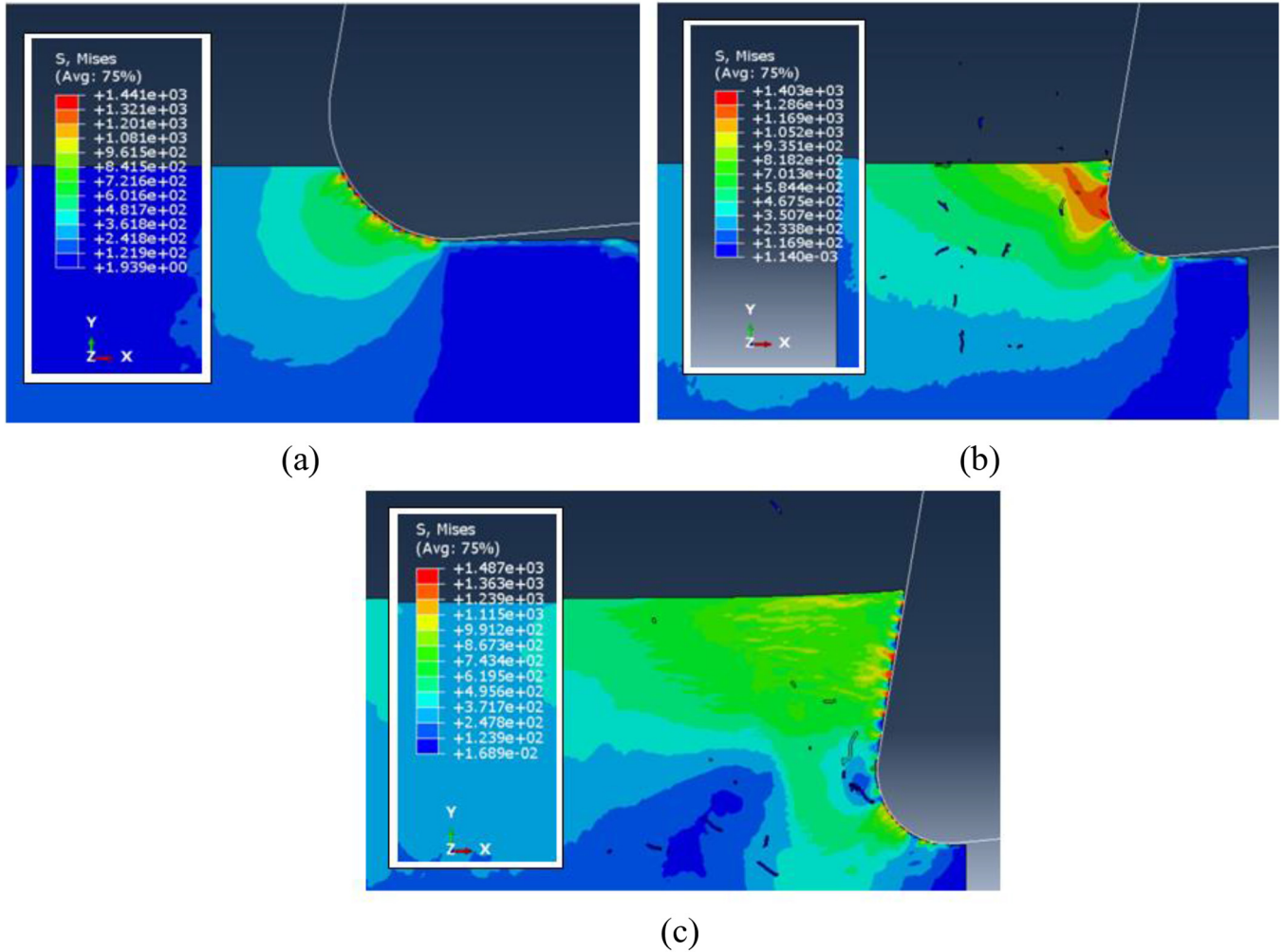
**Fig. 3.** Micro end milling process with two fluted end mill.

distribution at lower feed had shown higher value of stresses than the feed value equal to cutting edge radius i.e. 2 μm . The value of Von-Misses stress decreases as the feed approaches the cutting edge radius. This suggest at lower feed the phenomenon of ploughing is dominating. The ploughing or rubbing occurring at lower feed increases the stress values. When feed value equals to cutting edge radius, material removed by elasto-plastic deformation. Beyond 2 $\mu\text{m}/\text{tooth}$ feed, the value of stresses reduced significantly, this attributed for elimination of elastic deformation and removal of material entirely by plastic deformation. Further, by increasing the feed value above 3 $\mu\text{m}/\text{tooth}$ stress values increases considerably, increasing the chip load at higher feed generates higher stress value similar to macromachining. The stress values obtained after 4 $\mu\text{m}/\text{tooth}$ are higher than the stress value obtain at low feed (0.5 $\mu\text{m}/\text{tooth}$).

Tangential force (F_t) and feed force (F_f) are calculated by using equations (4) and (5) given below. F_x and F_y are the simulated force along X and Y direction respectively. φ is the positioning or rotation angle of end mill flute. Figure 6 shows the variation in tangential force and feed force with feed. At lower feed no significant variation in cutting force has been found, but the values of cutting forces reducing as the provided feed value approaching the cutting edge radius. Higher value of cutting forces for feed

Table 3. Cutting parameters used for FEM simulation of micro end milling.

Cutting parameter	Units	Value
Spindle speed (N)	RPM	60,000
Feed rate (f_t)	$\mu\text{m}/\text{tooth}$	0.5, 1.0, 1.5, 2.0, 2.5, 3.0, 4, 5, 6
Depth of cut (d)	μm	50

**Fig. 4.** Predicted Von-Mises stress distribution at spindle speed of 60,000 rpm, depth of cut 50 μm and (a) 0.5 $\mu\text{m}/\text{tooth}$, (b) 3 $\mu\text{m}/\text{tooth}$ and (c) 6 $\mu\text{m}/\text{tooth}$.

0.5 $\mu\text{m}/\text{tooth}$ – 1.5 $\mu\text{m}/\text{tooth}$ suggests the occurring of ploughing at low feed values. As the provided feed increased beyond 2 $\mu\text{m}/\text{tooth}$, ploughing eliminated and chip produced by plastic deformation. As the feed increases 3 $\mu\text{m}/\text{tooth}$ to 6 $\mu\text{m}/\text{tooth}$ the values of tangential force increases directly with feed. The rate of change of tangential force with feed significantly higher than feed force. The values of feed force are increasing slightly with feed. Increased values of tangential force with feed attributed to increase in chip load at higher feed. The value of feed slightly higher than cutting edge radius

producing lower value of cutting forces.

$$F_y = F_t \sin \varphi - F_f \cos \varphi \quad (4)$$

$$F_x = -F_t \cos \varphi - F_f \sin \varphi \quad (5)$$

To study the size effect in micro end milling process, specific cutting force was calculated by dividing the tangential and feed force by the product of chip load and axial depth of cut. In Figure 7 it is found the value of specific cutting force increased with decrease in the ratio of

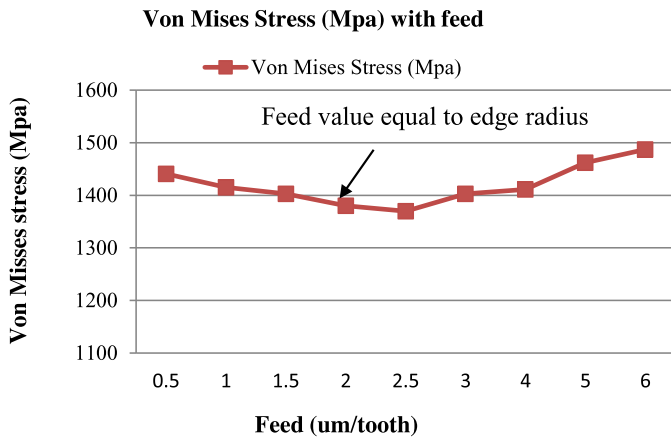


Fig. 5. Variation of maximum Von-Mises stress with feed.

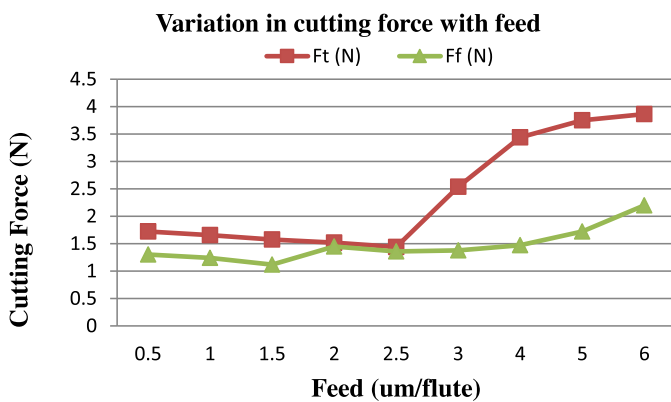


Fig. 6. Variation in tangential force (F_t) and feed force (F_f) with feed (simulated results).

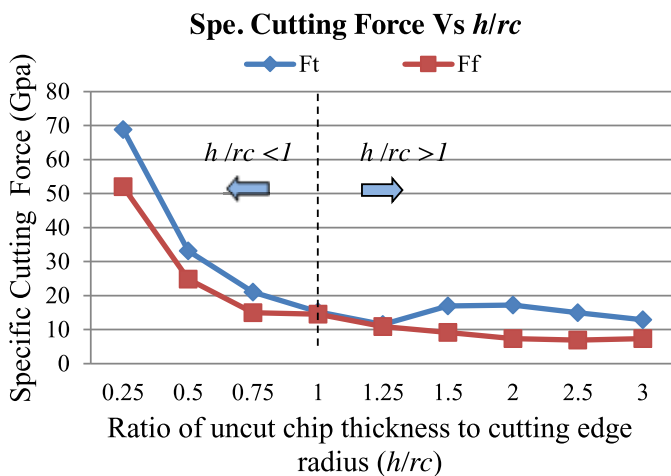


Fig. 7. Variation in specific cutting forces with ratio of undeformed chip thickness to cutting edge radius.

undeformed chip thickness to cutting edge radius. Higher values of specific cutting force has been observed when ratio of undeformed chip thickness to cutting edge radius was less than 1, this suggest the ploughing occurred at low

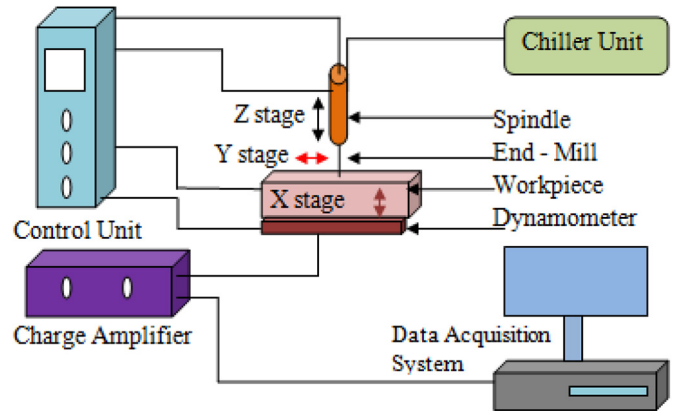


Fig. 8. Schematic representation of high speed micro end milling set up.

feed rate. This trend of specific cutting force shows agreement with results obtained by Aramcharoen and Mativenga [6].

3 Experimental validation

In this section, the details of workpiece material, cutting parameters, micro milling set up and measurement of cutting force has been presented. Simulated and experimental cutting forces are compared and percentage error calculated. Further, the surface roughness of machined slots measured and effect of different ratio of h/rc on Ra has been presented.

3.1 Experimental details

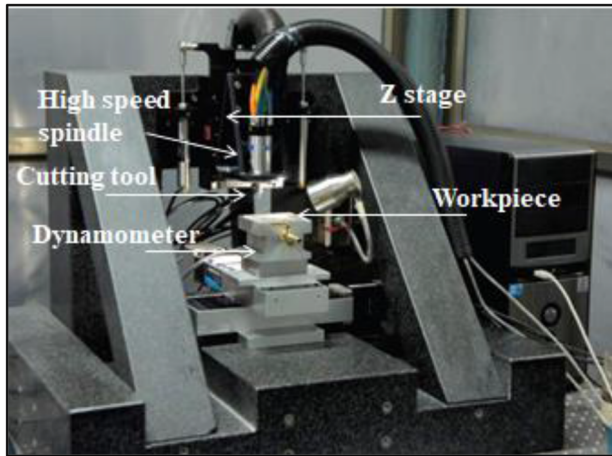
Schematic representation of high speed micro end milling set up is shown in Figure 8. In present study, Ti-6Al-4V (grade 5) workpiece with dimension $60 \times 40 \times 5$ mm has been used.

Axis made micro tungsten carbide end mill with diameter $800 \mu\text{m}$ and 10% of cobalt binder has been used for cutting in dry environment. Slots of 20 mm length and $800 \mu\text{m}$ diameter are cut on workpiece. Kistler made minidyne 9256C1 dynamometer has been used to measure the cutting forces. The cutting forces while milling measured by fixing the workpiece on the top of dynamometer. Three dimensional Alicona surface profilometer has been used to measure the surface roughness (Ra). Surface roughness is measured at two locations on machined slot i.e. at the starting and ending of the slot and average of that value taken as final Ra value for the respective experiment. Cutting parameters used to produce the slots on Ti-6Al-4V workpiece are presented in Table 4.

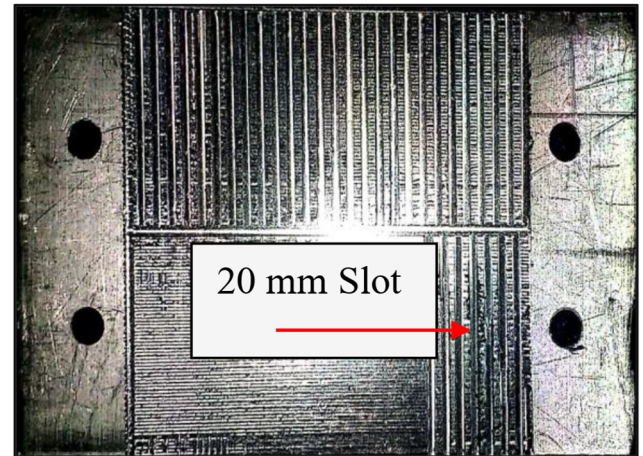
The actual experimental set up used in proposed work shown in Figure 9a while Figure 9b shows the machined slots on Ti-6Al-4V workpiece. High speed micro milling set up designed and developed by IIT Bombay has been used for machining. It has maximum 140,000 rpm spindle speed and average torque of ~ 4.3 N-cm. All three stages are mounted on granite rigid structure. The whole

Table 4. Cutting parameters used for micro end milling.

Cutting parameter	Units	Value
Spindle speed (N)	RPM	60,000
Feed rate (f_t)	$\mu\text{m}/\text{tooth}$	0.5, 2, 2.5, 4
Depth of cut (d)	μm	50



(a)



(b)

Fig. 9. (a) Micromilling set up and (b) machined Ti-6Al-4V alloy.

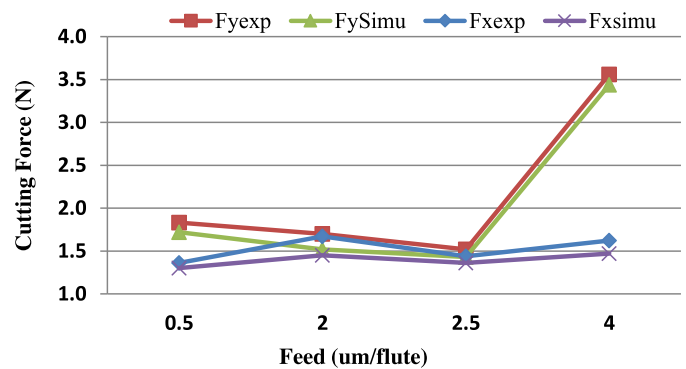
micromachining center is placed on the vibration isolation table. The x - y stages are actuated by ball screw mechanism driven by a DC brushless servomotor.

3.2 Model validation

To check the predictability of proposed model, the experimental F_y (force normal to feed) and F_x (force along feed) are compared with simulated forces. The simulated and experimental forces at cutting speed 60000 rpm, depth of cut 50 μm and feed 0.5, 2, 2.5 and 4 $\mu\text{m}/\text{tooth}$ are compared in Figure 10.

It is found that the predicted and experimental cutting forces are in good agreement. However, small difference between the values of simulated and experimental forces can be attributed to the tool wear, tool dynamics and small defects (crystal defects and impurities) associated with workpiece material. As in present work tool is considered as rigid body and defects associated with material are difficult to eliminate. Moreover, in actual machining tool wear and tool dynamics causes variation in cutting forces.

Table 5 shows the experimental and simulated cutting force values by considering the average of peak values of cutting force. It also shows the error between predicted and experimental cutting force. The maximum and minimum error for F_y is 11.84 and 3.57% respectively. Similarly the maximum and minimum error for F_x is 15.17 and 4.61% respectively.

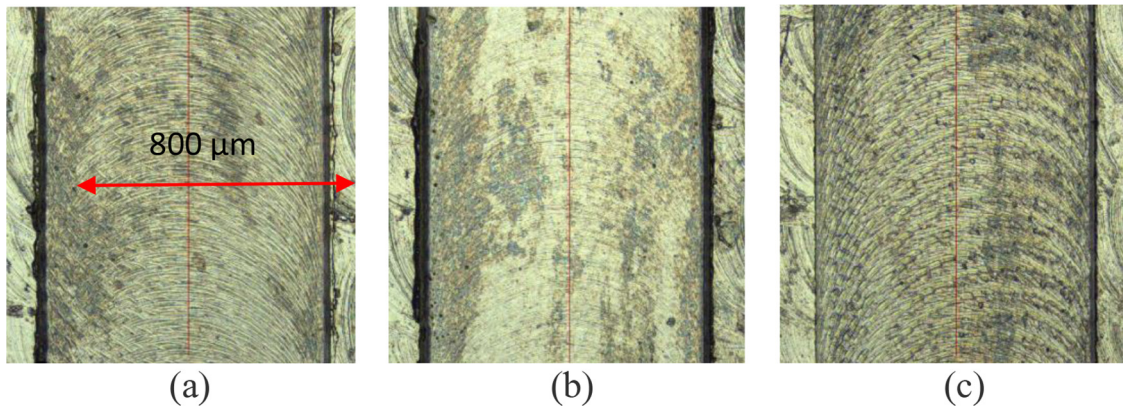
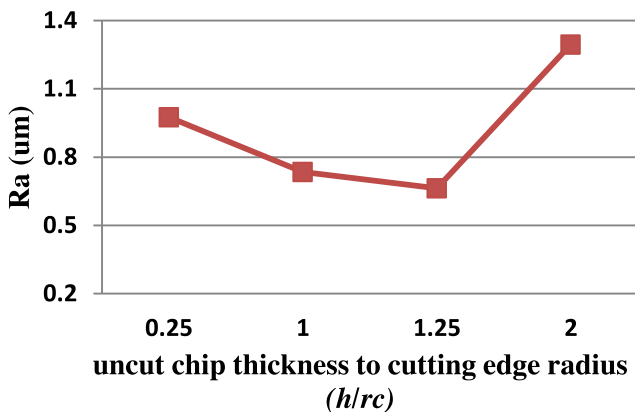
**Fig. 10.** Comparison of experimental and simulated cutting force at cutting speed 60,000 rpm, depth of cut 50 μm and feed 0.5, 2, 2.5, 4 $\mu\text{m}/\text{tooth}$.

In micro milling, low values of feed deteriorate the surface by ploughing, whereas higher value of feed may increase the surface roughness by increasing chip load [6]. Therefore, to identify the right h/rc ratio, Ra value of selected machined slots has been measured. Figure 11 shows the machined slot of 0.25, 1.25 and 2 h/rc ratio respectively and Figure 12 shows the effect of different h/rc ratio on Ra.

Figure 12 shows as the h/rc ratio approaching to the unity, the value of surface toughness decreasing. Just beyond the unity the obtained Ra value is significantly

Table 5. Experimental and simulated cutting force value.

Cutting condition			Average of peak values of cutting force F_y (N)			Average of peak values of cutting force F_x (N)		
Cutting speed (N)	Depth of cut (d) (μm)	Feed rate (f_t) ($\mu\text{m}/\text{tooth}$)	Experimental	Simulated	Error (%)	Experimental	Simulated	Error (%)
60,000	50	0.5	1.83	1.72	6.39	1.36	1.30	4.61
		2	1.70	1.52	11.84	1.67	1.45	15.17
		2.5	1.52	1.43	6.29	1.44	1.36	5.88
		4	3.56	3.43	3.57	1.62	1.47	10.43

**Fig. 11.** Machined slot for h/rc ratio (a) 0.25 (b) 1.25 (c) 2.**Fig. 12.** Effect of uncut chip thickness to cutting edge radius ratio on surface roughness (Ra).

lower, while at $2 h/rc$ ratio the higher value of surface roughness has been observed. The Ra value obtained at $0.25 h/rc$ ratio is significantly affected by ploughing mechanism, [Figure 11a](#) shows the elastically deformed marks on the machined surface. At $1.25 h/rc$ ratio, the

elastic deformation of material eliminated entirely and material removed by plastic deformation. At unity ratio, material removed by elastic-plastic deformation this attributed to little higher value of Ra at unity than $1.25 h/rc$ ratio. [Figure 11b](#) shows the machined slot at $1.25 h/rc$ ratio, the obtained surface has quite less roughness value. Similarly [Figure 11c](#) shows the surface obtained at $2 h/rc$ ratio, the Ra value obtained at this ratio is significantly higher. The unsymmetrical feed marks on the machined surface suggest the generation of high cutting forces at higher feed/tooth. The increased chip load at higher feed leads to high tool deflection, chatter and tool run out. Feed/ tooth is one of the significant parameter for surface roughness. Higher feed value increases the tool wear which leads to rounding of cutting edge and geometrical inaccuracies. In the present work cutting edge radius is $2 \mu\text{m}$, therefore the provided feed around $2.5 \mu\text{m}/\text{tooth}$ (h/rc ratio is 1.25) is suitable to produce lower surface roughness value. The obtained results shows agreement with recommendation given by *K and Mathew's* while micromilling of Ti-6Al-4V [25] according to them to optimize the surface roughness the selection of feed/tooth slightly higher than cutting edge radius is appropriate.

4 Conclusion

The ratio of uncut chip thickness to cutting edge radius is one of the significant parameter in micro milling. The appropriate selection of this ratio can reduce the cutting forces, surface roughness and tool wear by avoiding ploughing mechanism and over chip load. Limited application of FEM has been observed to predict ratio of uncut chip thickness to cutting edge radius in micro milling. Therefore in present work, the model developed by ABAQUAS/Explicit 6.12 used to predict the cutting forces while machining Ti alloy by using Johnson-Cook equation. The proposed model shows the effect of different feed on Von-Misses stress, tangential force and feed force. The effect of different h/rc ratio on surface roughness and specific cutting force also has been studied. On the basis of conducted study following conclusion can be drawn.

- Lower value of Von-Misses stress generates on machined surface and it increases toward cutting edge of the tool. Higher force required at cutting edge to produce the chip in cutting zone.
- As the feed value approaches the cutting edge radius ploughing avoided and just beyond cutting edge radius material removed completely by plastic deformation. Tangential force increased with feed after $3\ \mu\text{m}/\text{tooth}$, this attributed to increase in chip load at higher feed. The rate of change of tangential force considerably higher than feed force.
- FEM simulation for Von-Misses stress and specific cutting force shows size effect at lower feed.
- Cutting forces predicted by FEM simulation are in good agreement with experimental forces. Forces predicted by FEM model are 85–96% confidence level.
- To optimize the surface roughness, set the feed per tooth value slightly higher than cutting edge radius of the tool. At this feed elastic, elastic-plastic deformation eliminated completely and material removed by plastic deformation. In the present work, the provided feed around $2.5\ \mu\text{m}/\text{tooth}$ (h/rc ratio is 1.25) is found suitable to produce optimum surface finish and cutting forces.

References

1. M.A. Camara, J.C. Rubio Campos, A.M. Abrao, J.P. Davim, State of the art on Micromilling of material: a review, *J. Mater. Sci. Technol.* **28**, 673–685 (2012)
2. R. Mittal, S. Kulkarni, R. Singh, Effect of lubrication on machining response and dynamic instability in high-speed micromilling of Ti-6Al-4V, *J. Manufactur. Process.* **28**, 413–421 (2017)
3. M. Rahman, A.S. Kumar, J.R.S. Prakash, Micro milling of pure copper, *J. Mater. Process. Technol.* **116**, 39–43 (2001)
4. F. Ducobu, E. Filippi, Rivie E re-Lorphever, Chip formation in micro-milling, in *Proceedings of the 8th National Congress on Theoretical and Applied Mechanics, May 28-29, Brussels, Belgium*, 2010, pp. 333–339
5. J. Chae, S. Park, T. Freiheit, Investigation of micro-cutting operations, *Int. J. Mach. Tools Manufact.* **46**, 313–332 (2006)
6. A. Aramcharoen, P.T. Mativenga, Size effect and tool geometry in micromilling of tool steel, *Precis. Eng.* **33**, 402–407 (2009)
7. G. Bissacco, H. Hansen, L. Chiffre, Micromilling of hardened tool steel for mould making applications, *J. Mater. Process. Technol.* **167**, 201–207 (2005)
8. B. Barnabas, G. Norbert, T. Marton, J. Davim, A review on micro-milling: recent advances and future trends, *Int. J. Adv. Manufactur. Technol.* **112**, 655–684 (2021)
9. X. Liu, R.E. Devor, S.G. Kapoor, K.F. Ehmann, The mechanics of machining at the micro scale: assessment of the current state of the science, *Trans. ASME J. Manuf. Sci. Eng.* **126**, 666–678 (2004)
10. D. Dornfeld, S. Min, Y. Takeuchi, Recent advances in mechanical micromachining, *Ann. CIRP Manuf. Technol.* **55**, 745–769 (2006)
11. P.J. Arrazola, T.O. zel, D. Umbrello, M. Davies, I.S. Jawahir, Recent advances in modelling of metal machining processes, *Ann. CIRP Manuf. Technol.* **62**, 695–718 (2013)
12. T. Thepsonthi, T. Ozel, 3-D finite element process simulation of micro-end milling ti-6al-4v titanium alloy: experimental validations on chip flow and tool wear, *J. Mater. Process. Technol.* **221**, 128–145 (2015)
13. A. Davoudinejad, P. Parenti, A. Annoni, 3D finite element prediction performance of chip flow, burr formation and cutting forces in micro end-milling of aluminum 6061-T6, *Front. Mech. Eng.* **12**, 203–214 (2017)
14. T. Pratap, K. Patra, Finite element method based modeling for prediction of cutting forces in micro-end milling, *J. Inst. Eng. (India) Series C* **98**, 17–26 (2017)
15. T. Thepsonthi, T. Ozel, Finite element simulation of micro-end milling titanium alloy: comparison of viscoplastic and elasto-viscoplastic models, *NAMRI/SME, Madison, Wisconsin* (2013), Vol. 41
16. A. Attanasio, A. Abeni, T. Ozel, E. Ceretti, Finite element simulation of high speed micro milling in the presence of tool run-out with experimental validations, *Int. J. Adv. Manufactur. Technol.* **100**, 25–35 (2019)
17. F. Wang, X. Cheng, Y. Liu, X. Yang, F. Meng, Micromilling simulation for the hard-to-cut material, *Proc. Eng.* **174**, 693–699 (2017)
18. T. Pratap, K. Patra, A.A. Dyakonov, Modeling cutting force in micro-milling of Ti-6Al-4V titanium alloy, *Proc. Eng.* **129**, 134–139 (2015)
19. X. Jin, Y. Altintas, Prediction of micro-milling forces with finite element method, *J. Mater. Process. Technol.* **212**, 542–552 (2012)
20. Y.M. Ahmed, K. S. M. Sahari, M. Ishak, A.B. Khidhir, Titanium and its alloy, *Int. J. Sci. Res.* **3**, 1351–1361, (2012)
21. D. Carou, E.M. Rubio, J. Herrera, C.H. Lauro, J.P. Davim, Latest advances in the micro-milling of titanium alloys: a review, in *Manufacturing engineering society international conference MESIC 2017, 28-30, Vigo, Pontevedra, Spain June 2017* (2017)
22. V. Bajpai, A. Kushwaha, R. Singh, Burr formation and surface quality in high speed micromilling of titanium alloy

- (Ti-6Al-4V), in *Proceedings of the ASME, International Manufacturing Science and Engineering Conference MSEC2013; 2013 June 10-14; Madison, Wisconsin, USA, 2013*
23. A. Dadgari, D. Huo, D. Swales, Investigation on tool wear and tool life prediction in micro-milling of Ti-6Al-4V, *Nanotechnol. Precis. Eng.* **1**, 218–225 (2018)
 24. H.B. Wu, S.J. Zhang, 3D FEM simulation of milling process for titanium alloy Ti-6Al-4V, *Int. J. Adv. Manuf. Technol.* **71**, 1319–1326 (2014)
 25. K. Vipindas, J. Mathew, Wear behavior of TiAlN coated WC tool during micro end milling of Ti-6Al-4V and analysis of surface roughness, *Wear* **424-425**, 165–182 (2019)

Cite this article as: Narendra Bhople, Sachin Mastud, Satish Satpal, Modelling and analysis of cutting forces while micro end milling of Ti-alloy using finite element method, *Int. J. Simul. Multidisci. Des. Optim.* **12**, 26 (2021)